Shape Characterization of Point Sets in 2D

Course Notes Prepared by
Jiju Peethambaran and Stefan Ohrhallinger and Amal Dev Parakkat

1. Problem Definition

Shape characterization of a two dimensional (2D) point set is a fundamental problem that has many applications in computer graphics [SCT*14], computer vision [CCP97], and geographical information science (GIS) [GD06]. Technologies such as GPS and applications in GIS acquire discrete point-like objects in the form of dot pattern in two or three dimensional space. Many GIS applications use the "outline" of a group of objects, e.g.,trees, buildings or a flock of birds, or generally of any aggregation of discrete objects [GD06]. In geometric modeling, boundary of the surface patch that satisfies certain geometric constraints is computed in the 2D parametric space of the surface [SCT*14]. When all the surface points that satisfy the geometric constraints are computed and transformed into the (u, v) space, this becomes a shape characterization problem. Shape reconstruction techniques can also be employed to better approximate the regions of interest in crash optimization problems [GRM15].

Inputs to the shape characterization problem is any finite set of points in 2D and the outputs are either a graph or polygon(s) defining the point set shape, see Figure 1. The input point sets are known as either region samples [GD06] or area samples [OPP*21] or dot patterns [CCP97]. Shape characterization or region reconstruction problem can be formally described as in Definition 1.

DEFINITION 1 Given a finite set of points, $S \subseteq R^2$ sampled from a region or object, shape reconstruction deals with computing a polygonal boundary that best characterizes the underlying shape of S.

The 'shape' of a point set is a vague notion and can have multiple interpretations, i.e., point set shapes are highly subjective in nature and often depend on human cognition and visual perception. Therefore, the shape (or outline) is not by any means uniquely determined. To demonstrate this, observe that each of the illustrations in Figure 2 represents a possible outline for the same set of points; depending on one's purpose in requiring an outline, some may be "better" solutions than others, but none is absolutely "correct" [GD06]. This makes it almost impossible to formally define the shape formed by a set of points. The rich variety of shapes available in the nature and the heterogeneity of point sets further weaken a well-defined formulation of the shape approximation problem [Ede98].

Galton et al. [GD06] propose a set of general criteria that may be considered while defining what constitutes an optimal shape of a set of points for a particular application. Let S be a set of points

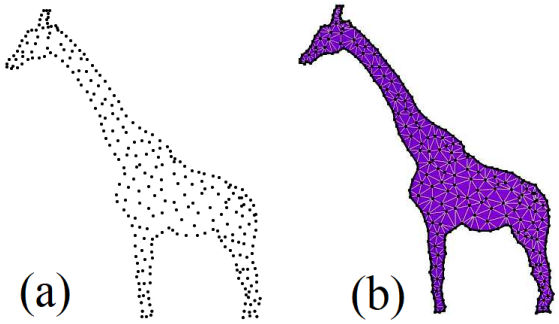

Figure 1: (a) Dot pattern, (b) Reconstructed shape, Image courtesy: [PM15a]

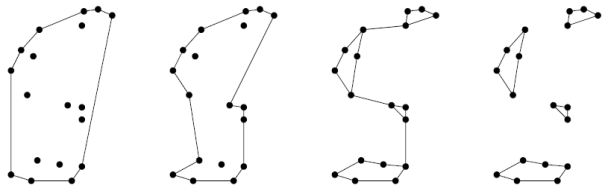

Figure 2: (Possible outlines for the region occupied by (or shape of) a set of points, Image courtesy: [GD06]

and $R(S)$ be the region occupied by S. The list of criteria are listed below.

- Should every member of S fall within R(S), as in Figure 3(a,c–g), or are outliers permitted, as in Figure 3(b)?
- Should any points of S be allowed to fall on the boundary of R(S), as in Figure 3(a–b,d–g), or must they all lie in its interior, as in Figure 3(c)?
- Should R(S) be topologically regular, as in Figure 3(a–c, e–g), or can it contain exposed point or line elements, as in Figure 3(d)?
- Should R(S) be connected, as in Figure 3(a–d,f,g), or can it have more than one component, as in Figure 3(e)?
- Should R(S) be polygonal, as in Figure 3(a–e,g), or can its boundary be curved, as in Figure 3(f)?
- Should R(S) be simple, i.e., its boundary is a Jordan curve, as

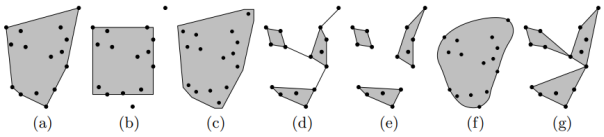

Figure 3: Illustration of point set with different aggregation patterns, Image courtesy: [GD06]

in Figure 3(a–c,f), or can it have point connections as in Figure 3(g)?

Depending on the application, the designers have the flexibility to impose the whole or a refined sub set of the above criteria to define the region or shape.

2. Classification

Broadly, the shape characterization algorithms are grouped into Delaunay based and non-Delaunay based algorithms.

2.1. Delaunay Filtration

In $\mathbb{R}^2$, α-shapes of a point set S is generated by connecting the points p,$q \in S$, which are touched by an empty disk of radius α [EKS83]. However, α-shape construction is parameterized in terms of α and there exists some point sets for which the α-shape family does not contain elements representing appropriate shapes [MD00]. To overcome the limitations of α-shape, Melkemi has introduced A-shapes which contains α-shape and crust as special cases [MD00]. Given a finite set of points P, and an arbitrarily chosen set A, A-shape of P is generated by first constructing the Voronoi diagram for $A \cup P$ and then joining together any pair of points p,$q \in P$ whose Voronoi cells both border each other and border some common Voronoi cell containing a point of A. However, determination of a proper A in A-shape computation is controlled by two parameters, α and t.

A related algorithm for characterizing a point set distribution is characteristic shape (or χ-shape) [DKWG08a]. χ-shape algorithm removes external edges of Delaunay triangulation until the largest edge on the boundary is less than a threshold value. Termination and efficiency of the algorithm and the boundary of χ-shape are dependent on the threshold value. Further, it generates only simply connected shapes (holes cannot be detected). Recently, variants of α-shapes such as k-order α-hulls [KPV10] and LDA-α-complex [CM11] have been proposed for shape reconstruction. LDA-α-complex effectively uses the local density variation found in the point sets for detecting the hollow regions.

Peethambaran et al. [PM15a] focus on the non-parametric approach that captures the topological properties of objects having directed boundary samples using Delaunay filtering. Methirumangalath et al. [MPM15] proposed a unified Delaunay-based framework for the reconstruction of a planar point set that is capable of detecting a wide variety of shapes having features such as sharp corners, concavities, thin regions etc. Focusing on boundary samples and dot patterns, Thayyil et al. [TPM20] proposed an input independent single-pass algorithm that removes edges based on characterizing a triangle by the distance between its circumcenter and incenter. Outer and inner boundaries of point sets are efficiently extracted using a Delaunay triangulation-based strategy in [MKPM17] that is capable of detecting sharp edges and holes.

2.2. Non-Delaunay based Methods

2.2.1. Region Approximation using Concave hulls

The work in this thesis can be related to the region approximations using concave hulls in computational geometry. Even though considerable amount of research has been done for reconstructing the region occupied by a set of points in the plane, all of them lack a concrete mathematical definition for concave hull and thus result in ambiguous representations for concave hulls of planar point sets. Junyi Xu et al. [XFZQ10] proposed ω-hull algorithm to compute concave hull for scattered data based on Graham scan convex hull algorithm. As the name suggests, the concave hull generated depends on the value of two externally supplied parameters, ω and ρ. A k-nearest neighbor algorithm for computing concave hull of point sets can be found in [MS07]. This is essentially a modified Gift wrapping algorithm which produces an envelope for a set of points where the shape of the envelope depends on the value of k. Galton et al. presented a swinging arm algorithm for the computation of region occupied by set of points in plane. The footprint obtained by Swinging Arm algorithm depends on the value of swinging arm, which is a line anchored to the last point added to the footprint (similar to half line in gift wrapping algorithm [O'R98]).

2.2.2. Proximity Graphs for Shape Characterization

In general, proximity graphs such as Relative neighborhood graph (RNG), Gabriel graph, Sphere-of-Influence graph [Tou88] and β-skeltons [KR85] play a vital role in defining the shape and structure of planar point sets [JT92].

In RNG, two points p and q are connected if $d(p,q) \leq d(p,x)$ and $d(p,q) \leq d(q,x)\ \forall\ x \in S$ where $x \neq p$ or q [JT92]. Gabriel graph of S contains all edges (p,q) where there exists an edge (p,q) if the circle passing through p and q centered at the edge (p,q) is empty [GS69].

Let S be a set of n points in the plane. For $p \in S$, let r_p be the minimum distance from p to $S-p$, and let B_p denote the open ball of radius r_p with center p, there exist an edge (p,q) in the sphere of influence graph of S, iff $d(p,q) \leq r_p + r_q$ [Tou88]. All these definitions may result in a graph rather than a simple polygon and hence may contain disconnected regions, isolated edges and junction points.

In β-skeleton, two points p and q, are connected to each other if there are two disks with radius $\beta \leq \frac{d(p,q)}{2}$ passing through them and is empty of other points of S [KR85]. In the γ-neighborhood graph is a generalization of β-skeleton in which there is no restriction on the radius of disks [Vel94]. In both these cases, an external parameter that must be fixed by a user to generate the graph. Moreover, if the original shape is not sampled uniformly or the parameter is not set appropriately, the algorithm may generate graphs with disconnected components.

2.2.3. Other Approaches

A related line of work is polygonal border extraction of dot patterns which are mainly used in pattern recognition and digital image processing [CCP97]. Chaudhuri et al. [CCP97] introduced two new constructs called as *s*-shape and *r*-shape for border extraction. In 1999, Gautam et al. [GC99] proposed a split and merge procedure for computing the polygonal border of a dot pattern. Their final polygonal border depends on the choice of the number of sides of final polygon(m) or the area of the polygonal border. Recently, a polygonal border reconstruction algorithm (simple shape) has been proposed by A.Gheibi et al. which works for both dot patterns and boundary samples [GDJ*11]. However, simple shape depends on a thresh hold parameter and lacks the ability to detect holes in the shapes.

3. Delaunay based Algorithms

In a survey on shape reconstruction, Edelsbrunner [Ede98] elaborates on how different shape reconstruction methods restrict the Delaunay complex to arrive at their respective shapes. We discuss some of the Dealaunay filtration algorithms for point set shape characterization. We have included three prominent algorithms in this field, i.e., α-shape and χ-shape and a few recent ones along with a few related sampling models commonly used for providing theoretical guarantees. Basic notations and symbols used for discussion are summarized in Table 1.

3.1. Simplicial Complex

As the concept of simplicial complex is used in a few reconstruction algorithms, we provide the basic definition of simplicial complex. A k-simplex is the non-degenerate convex hull of $k+1$ geometrically distinct points, $v_0, v_1, ..., v_k \in \mathbb{R}^d$ where $k \leq d$ [CDS13] (Definition 2).

DEFINITION 2 k-simplex (σ_k):
It is the intersection of all convex sets containing $(v_0, v_1, ..., v_k)$. i.e., $\sigma_k = \{x \in \mathbb{R}^d \mid x = \sum_{i=0}^{k} \alpha_i v^i$ with $\alpha_i > 0$ and $\sum_{i=0}^{k} \alpha_i = 1\}$

According to the Definition 2, vertex is 0-simplex, edge is 1-simplex, triangle is 2-simplex and tetrahedron is 3-simplex. The convex hull of any non-empty subset of the $(k+1)$ points that defines a k-simplex is referred to as a **face** of that simplex. Like simplices, vertex is a 0-face, edge is a 1-face and so on. A $(k-1)$-faces of a k-simplex is called as a **facet**.

DEFINITION 3 Simplicial complex [CDS13]:
A simplicial complex, $\mathcal{K}$ is a set containing finitely many simplices that satisfies the following two restrictions:

- $\mathcal{K}$ contains every face of every simplex in $\mathcal{K}$;
- For any two simplices, $\sigma, \tau \in \mathcal{K}$, their intersection $\sigma \cap \tau$ is either empty or a common face of σ and τ.

Line segments which do not belong to any triangle in a $\mathcal{K}_2$ are either bridges, dangling edges or disconnected line segments (see Figure 4(a)). In a simplicial 2-complex, if one or more triangles are attached to any other k-simplex (where $k = 1$ or 2) through only one of its vertices, then that vertex is termed as a junction point, i.e., the triangle(s) is(are) free to oscillate about its junction point (see Figure 4(a)).

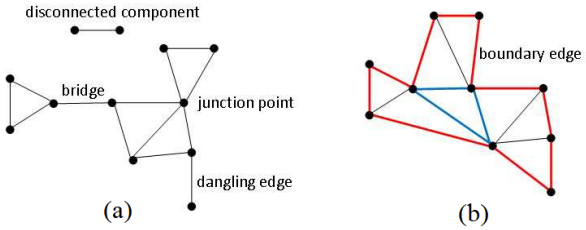

Figure 4: Illustration of regular and non-regular simplicial complexes. The constructs which violates the regularity of a graph are shown in Figure 4(a).

DEFINITION 4 Regular simplicial 2-complex ($\mathcal{RK}_2$):
A simplicial 2-complex $\mathcal{K}_2$ is said to be regular if it satisfies the following conditions:

- All the points in $\mathcal{K}_2$ are pairwise connected by a path on the edges.
- It does not contain any junction points, dangling edges or bridges.

A detailed explanation on simplices and simplicial complexes can be found in [CDS13]. An edge in $\mathcal{RK}_2$ is a boundary edge (red colored edges in Figure 4(b)) if it is incident to a single triangle.

DEFINITION 5 Boundary triangle:
A triangle in $\mathcal{RK}_2$ is a boundary triangle if it is incident to at least one boundary edge. In Figure 4(b), all triangles having red edges are boundary triangles.

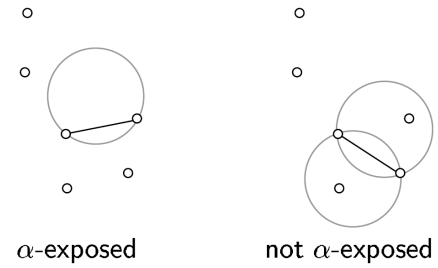

Figure 5: Illustration of α-exposed simplices, Image courtesy: [Fis].

3.2. α-shape [EKS83, EM94, Fis]

Conceptually, α-shape are presented as a generalization of the convex hull of a point set. We reproduce the definition of α-shape provided in [Fis].

DEFINITION 6 For $0 < \lambda < \infty$, let an λ-ball be an open ball with radius λ. Furthermore, a 0-ball is a point and an 1-ball is an open half-space. Now, a certain λ-ball b (at a given location) is called empty if $b \bigcap S = \phi$. With this, a k-simplex σ_k is said to be α-exposed (see Figure 6) if there exists an empty α-ball with $\sigma_k = \partial b \cap S$ where ∂b is the surface of the circle (d = 2) bounding b, respectively.

With this preliminaries, let us present the definition of α-shape, see Definition 7.

O	A shape	$d(u,v)$	The euclidean distance between the points u&v.
S	A finite set of points of O in R^2.	$\|\|x\|\|$	The length of x.
$DT(S)$	Delanauy triangulation of S [O'R94].	$deg(v)$	degree of vertex v.
$V(S)$	Voronoi diagram of S [O'R94].	∂O	Shape boundary.
$B(r,x,y)$	Ball having radius r passing through two distinct points x,y	$conv(.)$	Convex hull.

Table 1: Notation and Symbols

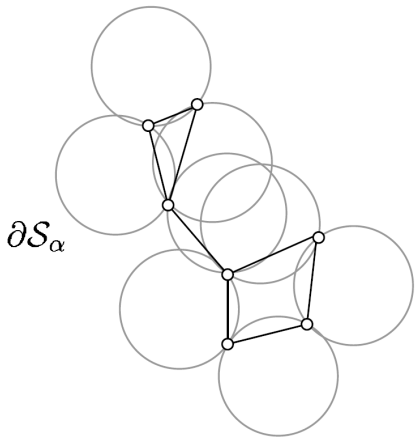

Figure 6: An example of alpha shape boundary, Image courtesy: [Fis].

DEFINITION 7 The boundary ∂S_α of the α-shape of the point set S consists of all k-simplices of S for $0 \leq k < d$ which are α-exposed,

$$\partial S_\alpha = \{\sigma_k \mid k \leq d, (v_0, v_1, ..., v_k) \subseteq S \text{ and } \sigma_k \text{ are } \alpha - exposed\}$$

Edelsbrunner et al. [EKS83] has shown that the boundary ∂S_α of the α-shape is a subset of the Delaunay triangulation of S for any value $0 < \alpha < \infty$. This relation has been utilized to design a linear algorithm for extracting α-shape from $DT(S)$.

3.3. $\mathcal{A}$-shape [MD00]

Melkemi presented a general family of shapes that includes α-shapes as a special case. A member in this family is identified with the help of a second finite set $\mathcal{A} \subseteq R^2$. The $\mathcal{A}$-shape of S is generated by drawing an edge connecting points $p,q \in S$ if there is a circle that passes through p,q, and a point $a \in \mathcal{A}$, and all other points of $S \bigcup A$ lie strictly outside the circle. The α-shape is the special case where $\mathcal{A}$ is the collection of points a on Voronoi edges that span empty circles of radius α with points in S. Melkemi suggests a two-parameter family of point sets, $\mathcal{A} = \mathcal{A}(\alpha, t)$. The first parameter, $\alpha \geq 0$, controls the resolution and the second parameter, $t \in [0,1]$, interpolates between the unweighted case and the case where points are weighted by the local density.

3.4. χ-shape [DKWG08b]

The *chi*-algorithm possibly yields a non-convex, simple polygon that characterizes the shape of a set of input points S in the plane. Characteristic shapes are simple (Jordan) polygons,homeomorphic to the closed unit disk. Thus, characteristic shapes are simply connected (all of one piece containing no holes nor islands) and regular. Characteristic shape is generated by repeatedly "removing" longest exterior edges (longer than a threshold l) from $DT(S)$ subjected to the regularity constraints. The resultant graph is always regular simplicial 2-simplex. Figure 7 shows a comparison between α-shape and χ-shape.

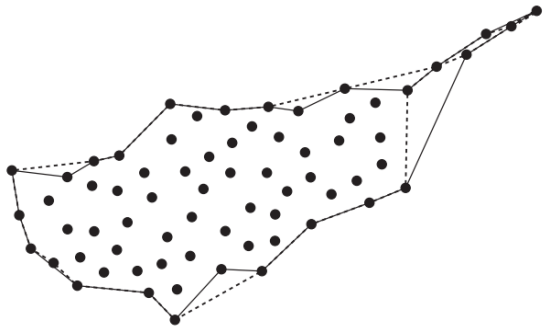

Figure 7: Example differences between alpha-shape (solid hairline) and chi-shape (thick dashed line), Image courtesy: [DKWG08b]

The χ-shape produced by the algorithm has the following properties.

- it is a simple polygon;
- it contains all the points of S; and
- it bounds an area contained within and possibly equal to the convex hull of the points of S.

3.5. Divergent Concavity of Object Boundaries

We review "divergent concavity" before providing the next few shape characterization algorithms. A closed planar curve that represents the boundary of an object is considered through out this section for illustration. A simple closed curve Σ bounds a region referred to as interior of Σ ($I(\Sigma)$), that lies to the left when travelled in counter clockwise direction along Σ. Jordan curve theorem establishes that a simple closed curve divides the plane into a well-defined interior ($I(\Sigma)$) and exterior ($\overline{I(\Sigma)}$).

Curve Σ is said to be **convex**, if the line segment between any two points on the curve falls in the interior, $I(\Sigma)$. Otherwise it is **concave**. The curvature κ at a point p of Σ is the rate of change of direction of the tangent line at p with respect to arc length s. An inflection point (IP) on the curve is a point where $\kappa = 0$ but $\kappa^{'} \neq 0$ (Figure 8). Since reconstruction in the presence of concave portions

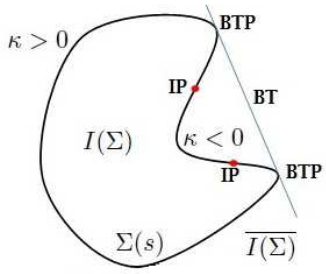

Figure 8: Inflection points (IP) and concave portions.

is extremely difficult, we restrict our attention to concave curves. Concave portions of a curve is characterized by the sign of the local curvature κ. Concave portions exists between two inflection points and has a negative local curvature sign ($\kappa < 0$).

A bi-tangent (BT) to a curve Σ is a tangent line L that touches Σ at two distinct points. The points where BT touches Σ is referred to as bi-tangent points (BTP). We consider only the bi-tangents lying completely in the exterior of the curve ($\overline{I(\Sigma)}$) for our discussion (i.e. BT refers to exterior bi-tangent). With these basic terminology, we introduce the definition of pseudo-concavity of Σ.

DEFINITION 8 Pseudo-concavity:
The portion of Σ lying between two bi-tangent points having at least one sub-portion with $\kappa < 0$ is called as pseudo-concave portion of Σ, denoted by $\mathcal{C}(\Sigma)$.

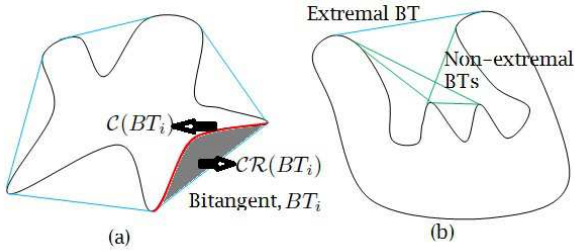

Figure 9: Illustration of pseudo-concave region ($\mathcal{CR}(BT_i)$, grey color region in Figure 9(a)), pseudo-concave portion ($\mathcal{C}(BT_i)$, red color curve portion shown in Figure 9(a)), extremal bi-tangent (blue color) and non-extremal bi-tangents (green color in Figure 9(b)).

Red colored portion of the curve in Figure 9(a) is an example of pseudo-concave portion. Here are some observations on pseudo-concavity of a curve (Figure 9).

1. Multiple pseudo-concave portions are possible for Σ.
2. A pseudo-concave portion $\mathcal{C}(\Sigma)$ always contains portions with $\kappa > 0$.
3. Every BT induces a $\mathcal{C}(\Sigma)$. The region bounded by BT and the corresponding $\mathcal{C}(\Sigma)$ constitutes the pseudo-concave region of BT, denoted by $\mathcal{CR}(BT)$ (grey colored region in Figure 9(a)).
4. There may exist some BT_i in $\mathcal{CR}(BT_j)$. Here, BT_i is referred to as non-extremal BT (green color bi-tangents in Figure 9(b)).

Medial axis of Σ is closure of the set of points in the plane which have two or more closest points in Σ [ABE98]. Medial axis also contains the centers of all osculating disks (empty disks tangent to Σ). A medial ball $B(c,r)$, centered at $c \in$ medial axis of Σ with radius r, is a maximal ball whose interior contains no points of Σ. For any Σ, there exists inner and outer medial axis. We restrict our attention to outer medial axis and the corresponding medial balls for defining divergent pseudo-concavity.

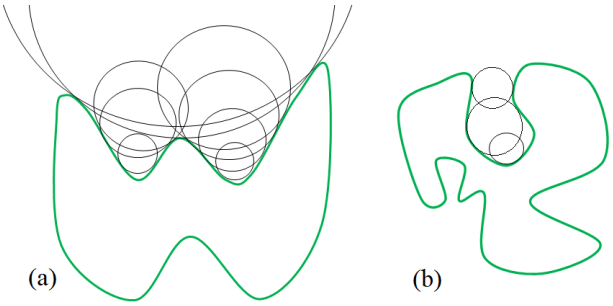

Figure 10: Illustration of divergent and non-divergent pseudo-concavities.

DEFINITION 9 Divergent pseudo-concavity:
A $\mathcal{C}(\mathcal{BT})$ of Σ is said to be divergent, if the radii of medial balls, $B(c,r)$, r_i monotonically increases as it goes along the outer medial axis of $\mathcal{C}(\mathcal{BT})$ from one end to the extremal BT end.

An example of divergent pseudo-concavity is illustrated in Figure 10(a). For $\mathcal{C}(\mathcal{BT})$ having non-extremal BTs, medial axis may have branches that go separately to different $\mathcal{C}(\mathcal{BT})$s of non-extremal BTs. The Definition 10 is valid in this case as well as the medial ball rolls only towards extremal BT end (Figure 10(a)).

DEFINITION 10 Divergent concave curve(Σ_D):
A simple, closed planar curve Σ is said be divergent concave if all its pseudo-concave portions ($\mathcal{C}(\mathcal{BT})$) are divergent.

Figures 10(a) & 10(b) illustrate examples of divergent and non-divergent curves respectively. In Figure 10(b), radii of medial balls continuously increase for some time, then decrease for a smaller interval of time and then again start increasing as the it approaches the corresponding extremal bi-tangent. There are other type of non-divergent pseudo-concavity where the radii of medial balls monotonously decreases as it approaches the extremal bi-tangent.

3.6. Relaxed Gabriel Graph [PM15a]

A relaxed Gabriel graph (RGG(S)), is a regular simplicial 2-complex that consists of most of the Gabriel edges and a few non-Gabriel edges inherited from the $DT(S)$. RGG(S) retains a non-Gabriel edge $(p,q) \in DT(S)$ if it satisfies either of the following:

- Circumcenter of the Delaunay triangle $\triangle pqr$ for which (p,q) is the characteristic edge, lies internal to $\partial RGG(S)$.
- Removal of (p,q) violates regularity in RGG(S).

RGG algorithm filter the boundary triangles subjected to regularity and circumcircle constraints. While regularity constraints ensure that the resultant graph is always a regular simplicial complex,

circumcenter constraint allows the removal of boundary triangles whose circumcenter lies outside of the intermediate boundary of the simplicial complex. Holes in the point sets are characterized using structural patterns formed by fat and thin Delaunay triangles.

Next we present a sampling model used to provide the theoretical guarantees on RGG algorithm. Let B is a set of points sampled from ∂O and $Del(B)$ denotes its Delaunay Graph., an **external Delaunay triangle** is a triangle, $\triangle_x \in Del(B)$ which is partially or fully exposed to the exterior of ∂O.i.e. $\{\triangle_x\} \cap \{\overline{I(\Sigma)}\} \subseteq \{\triangle_x\} \setminus \{\}$, where $\{\}$ is the null set. External Delaunay triangles exist in the pseudo-concave regions.

DEFINITION 11 Divergent boundary sample:
A point set B sampled from a divergent concave curve.

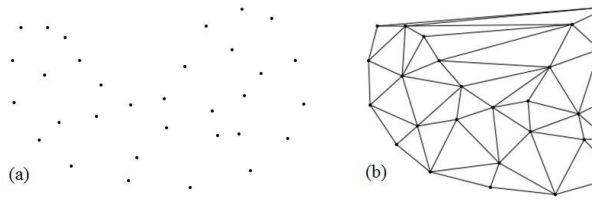

Figure 11: Illustration of Observation 1.

OBSERVATION 1 Every external Delaunay triangle in a divergent boundary sample is obtuse with its longest edge facing towards the extremal bi-tangent of the corresponding pseudo-concavity.

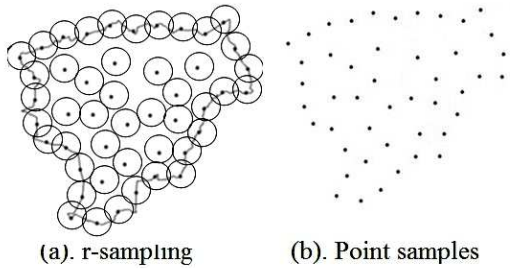

Figure 12: Illustration of a r-sampling using balls of radius r and the resultant point set of an object

3.6.0.1. $(r,\uparrow)$**-sample** In Definition 11, we considered only the boundary sample. Now we extend the definition to object samples with some additional sampling criteria. Sampling such as ε-sampling [ABE98], defined in terms of the medial axis of the object, enables providing theoretical guarantees for curve or surface reconstruction. ε-sampling to object samples seems to be inappropriate, as the points are distributed all over the object. So, We adopt a model similar to the one used in [Att98] with few additional constraints (Definition 12).

DEFINITION 12 $(r,\uparrow)$-sample:
A point set S sampled from a geometric object O is said to be $(r,\uparrow)$-sample if it satisfies the following properties.

1. Object O possesses a divergent concave boundary.
2. Each pair of adjacent boundary samples, $p,q \in \partial S$ lies at a distance of at most $2r$. i.e $d(p,q) \leq 2r$.
3. Each pair of samples p,q where $p \in int(S)$ and $q \in S$ lies at a minimum distance of $2r$, i.e $d(p,q) \geq 2r$.

The radius of the sampling balls r, can be chosen so that the balls fully cover the boundary of the object as shown in Figure 12. Interior of the object is sampled using the balls of same radius but the locations of the balls are arbitrary. The author(s) [PM15a] have provided theoretical analysis of RGG algorithm under $(r,\uparrow)$-sampling model.

3.7. EC-shape [MPM15]

In [MPM15], a unified algorithm for the reconstruction from boundary samples as well as dot patterns is proposed. The authors use circle constraint and regularity constraint for the Delaunay triangle filtration. Circle constraint is defined as follows.

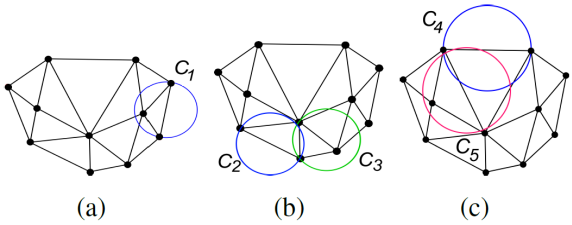

Figure 13: (a) Non-empty diametric circle C1 (b)Empty diametric circle C2 and non-empty chord circle C3 (c)Empty diametric circle C4 and non-empty midpoint circle C5 [MPM15]

DEFINITION 13 Circle Constraint - The exterior edge of a graph is said to satisfy circle constraint if any one of the following conditions is satisfied:

- Diametric circle (say, radius R) of the exterior edge of the graph is non-empty (i.e., the circle contains at least one point of S).
- Any chord circle with the same radius R for any of the adjacent sides of the exterior triangle is non-empty (a chord circle is available when $2R >$ the length of the adjacent side).
- Any midpoint circle with the same radius R for any of the adjacent sides of the exterior triangle is non-empty (a midpoint circle is available when chord circles are not available ie. when $2R <=$ length of the adjacent side).

Definition 13 utilizes three different types of circles namely diametric circle, chord circle and midpoint circle, see Figure 13. A Chord circle of an edge e_{ij} is a circle with e_{ij} as its chord, a midpoint circle of an edge e_{ij} is any circle whose centre is the mid point of the edge, and a diametric circle of an edge e_{ij} is a midpoint circle with diameter $\|p_i - p_j\|$. Please note that *exterior edge* and *exterior triangle* have the same definition as *boundary edge* and *boundary triangle* presented in Section 3.1.

EC-shape algorithm successively removes the boundary edges subject to regularity and circle constraints to compute the resultant boundary. Figure 14 illustrates the edge filtration of the EC-shape

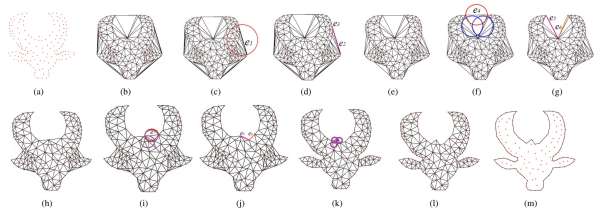

Figure 14: Different stages of ec-shape algorithm, Image courtesy: [MPM15]

algorithm. Under $r--$-sampling, Lemmas 4.1 and 4.2 of [MPM15] together establish that EC-shape is homeomorphic to a simple closed curve.

3.8. CT-shape [TPM20]

The CT-shape algorithm is an single-pass and input-independent (unified) reconstruction algorithm. The algorithm is said to be single-pass because it employs same strategy for capturing boundaries irrespective of the number of holes/objects. The definition of CT-shape utilizes different types of triangles, degree constraints, and pseudo hole.

DEFINITION 14

- Neighboring Triangles: Two triangles are said to be neighboring triangles if they share an edge (Figure 15(a)).
- Coordinated Triangles: Neighboring triangles are termed as co-ordinated triangles if their circumcenters lie on the same side of the shared edge (Figure 15(b)).
- Skinny Triangles: A skinny triangle is a thin non-obtuse triangle whose base is smaller than the distance between the circumcenter and the incenter of the triangle (Figure 15(c)).

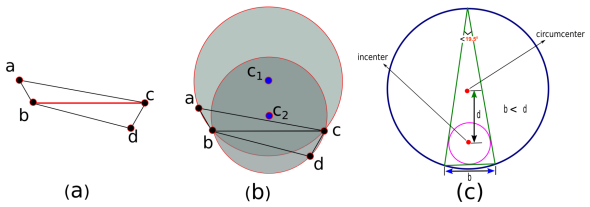

Figure 15: Illustration of definitions [TPM20]

DEFINITION 15 Degree constraint:
When there are more than two edges at a vertex (point), "degree constraint" implies that only two shorter edges are retained (and all other edges are removed) from that vertex (point).

Given $DT(S)$, CT-shape is constructed by marking all the shared edges from the coordinated triangles, and the two longer edges from the skinny triangles. Then create a new graph consisting of all the unmarked edges and imposing the degree constraints. The authors have provided topological correctness of CT-shape under r-sampling model.

3.9. Petal Ratio [TPM21]

A recent work [TPM21] in this direction attempts to discern the input type (curve sample or dot pattern) based on the notion of *Petal-Ratio (PR)* which is inspired by the flower structure mentioned in [PMM18]. The authors define *Petal-Ratio* as follows (Definition 16).

DEFINITION 16 Petal-Ratio(PR) : Let e_1 & e_2 are two of the edges incident with a vertex $v \in DT(S)$ such that e_1 is longest edge and e_2 is the smallest edge. Petal-Ratio of a vertex v is, $PR(v) = \frac{\|e_1\|}{\|e_2\|}$

Based on the idea of *Petal-Ratio (PR)*, an algorithm to extract the polygonal boundary of dot pattern along with theoretical guarantees under minimal reach sampling is provided.

3.9.1. Minimal Reach Sampling (MRS)

All the definitions are given under the assumption that the shape O possesses a smooth boundary ∂O which is equivalent to a smooth, possibly concave and closed curve. We utilize the notion of ***Pseudo concavity*** (Definition 8)to define minimal reach sampling. ***Local Feature size w.r.t exterior medial axis***, $lfs'(p)$, at a point $p \in \sum$ is the minimum Euclidean distance from the point p to a point $m \in M$, where M is the medial axis constituted by the union of outer medial balls.

Points in $\sum$ can be ordered either in clockwise or anti-clockwise direction. Based on one of these orderings, we say that a point $p \in \sum$ lies before or after another point $q \in \sum$. Such an oredring of curve points naturally leads to the concept of interval defined as follows. The interval $I(p) \equiv [p_0, p_1]$ is the set of curve points $p \in \sum$ between p_0 and p_1. ***Reach*** [Fed59] of a curve interval I can be defined as follows.

DEFINITION 17 Reach [Fed59] The reach of interval I is $inf_{p \in I} lfs(p)$

We slightly modify Definition 17 and adapt it to our setting. In particular, we consider the local feature size of points with respect to outer medial axes, not the inner medial axis. Hence reach of an interval I in this paper refers to $inf_{p \in I} lfs'(p)$. We consider the extremal bi-tangent points of pseudo-concavities as the end samples of different intervals. Essentially, each pseudo-concave portion is considered as a separate interval, i.e., pseudo-concave interval. We denote the set of reaches of all the pseudo-concave intervals of $\sum$ by R and find the minimum reach of pseudo-concavities (refer to Figure 17(a)), γ of $\sum$ by taking the minimum value from the set R (refer to Figure 17(b), $R = \{d_1(pink), d_2(red), d_3(blue)\}$ and γ of $\sum = min(R) = d_3$). Armed with these definitions, we formalize minimum reach sampling in Definition 18.

DEFINITION 18 Minimal reach sampling: A sampling S of shape O is said to be minimal reach sampling if the closest neighboring points with respect to any point $p \in S$ lies at a distance of exactly γ.

Minimal reach sampling is a special case of dense r-sampling [PM15b] where $r = \gamma$.

LEMMA 3.1 Let S be the minimal reach sampling of a shape O and $e_1, e_2 \in DT(S)$ be the shortest edge and an edge lying in a pseudo-concavity of ∂O from a boundary sample $v \in S$ respectively, then $\frac{\|e_2\|}{\|e_1\|} \geq 2$.

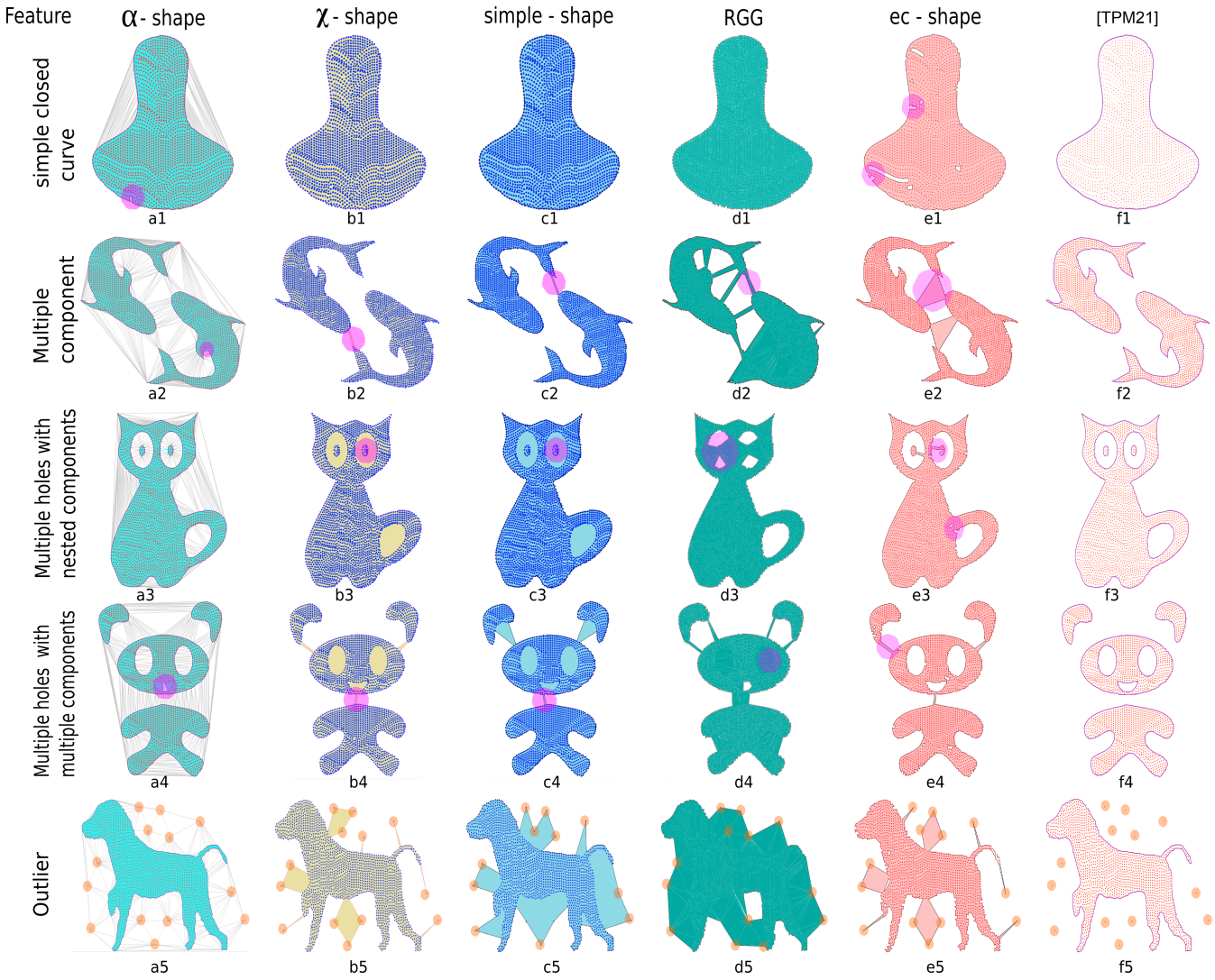

*Figure 16: A visual comparison of α-shape [EKS83], χ-shape [DKWG08a], Simple-shape [GDJ*11], RGG [PM15a], EC-shape [MPM15], and the results of [TPM21], Image Courtesy: [TPM21]*

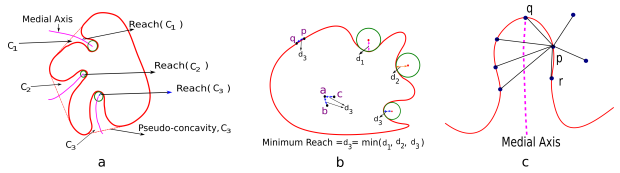

Figure 17: (a) Exemplification of minimal reach sampling (MRS) (b) Illustration of pseudo-concave reaches of a smooth curve (c) shows that Delaunay edges in the pseudo-concavities intersect the corresponding exterior medial axis. The dotted purple color curve indicates the exterior medial axis

Proof The minimal reach of ∂O, i.e., γ is the least external local feature size, $lfs(v)'$ of a boundary point v where v belong to one of the pseudo-concave portions of ∂O. In $DT(S)$, an edge (e_2) lying in the pseudo-concavity has a length of at least 2γ. This is due to the fact that all the Delaunay edges in the pseudo-concavities intersect the corresponding exterior medial axis (refer Figure 17(c)). According to minimal reach sampling, a boundary edge or a shape edge (both endpoints of an edge completely inside the boundary) can have a length of γ. So the shortest edge (e_1) from v has to be either a boundary edge or a shape edge. So we get $\frac{\|e_2\|}{\|e_1\|} \geq \frac{2\gamma}{\gamma} = 2$. □

Lemma 3.1 indicates that only those edges incident with a vertex, $v \in DT(S)$ having $PR(v) \leq 2$ are part of the shape O, where S conforms to a minimum reach sampling of O. This immediately gives us a simple algorithm to extract the polygonal border of dot patterns.

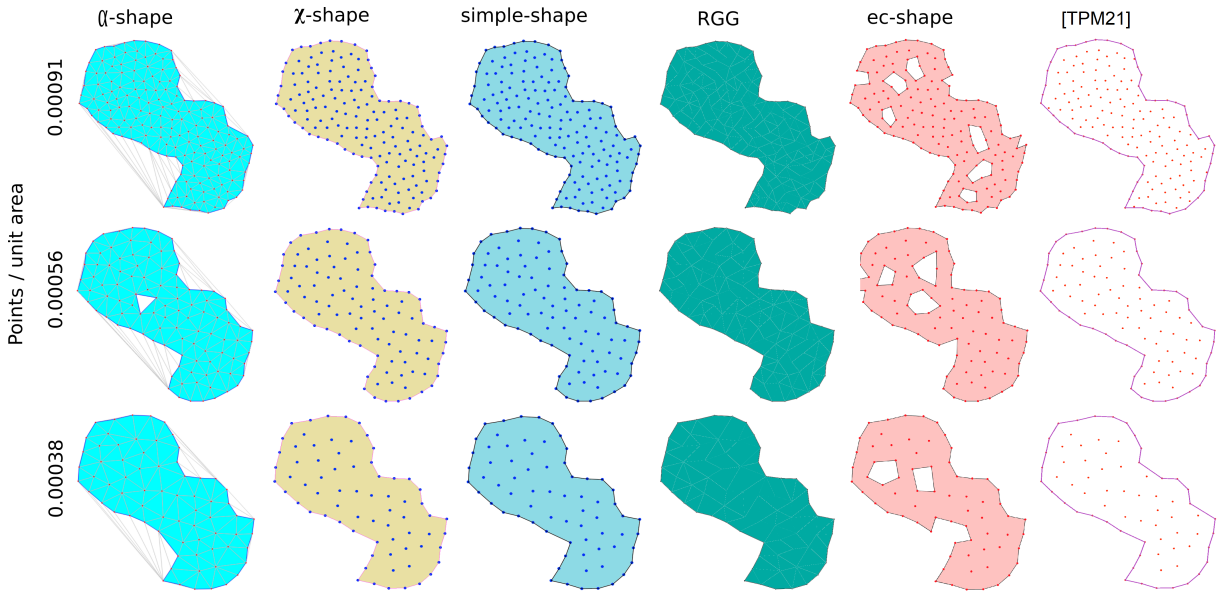

Figure 18: Shape characterizations by various algorithms for the map of the country, Paraguay, Image courtesy: [TPM21].

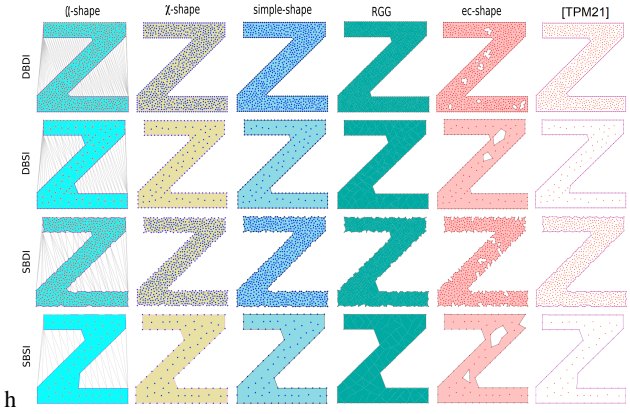

Figure 19: Effectiveness of different algorithms for inputs with varying point density, Image courtesy: [TPM21].

4. Evaluation Practices and Tools

4.1. Evaluation Criteria

In general, experimental evaluation of shape characterization algorithms are done using qualitative as well as quantitative analysis. The results are experimentally evaluated against a known original shape with respect to certain error parameters. Error is estimated as the area of symmetric difference between the original shape and the reconstructed result [DKWG08a]. The evaluation of the results are made extensive and authentic by carrying out experiments like varying point density and homogeneity in point distribution.

Quantitative analysis is done based on the L^2 error norm estimated as the area of symmetric difference between the original shape and the reconstructed result [DKWG08a]. Let $Area(O)$ and $Area(R(S))$ denote the area of the original shape and the area of the reconstructed shape respectively, then L^2 error norm is computed as in Equation 1.

$$L^2 \text{ error norm} = \frac{Area((O - R(S)) \bigcup (R(S) - O))}{Area(O)} \quad (1)$$

An L^2 error norm of zero implies that the two shapes are equal in area and also their boundaries are structurally alike. The units of the area in all the cases are square pixels.

Feature based Comparison. Typically, a visual comparison of various algorithmic results are performed for input shapes with different features, point samplings and distributions. Feature based evaluations include simple closed curves, multiple components, shapes with holes, and non-diverging concavity and outliers as shown in Figure 16.

Effects of Point Density. Another common experiment involves measuring how well the reconstruction algorithm behaves for different sampling density. Typically, shapes with highly sinusoidal boundary, e.g., country maps are selected for this experiment. points are semi-randomly sampled over the object or region. Shape reconstructions of objects with varying point densities (shown in Figure 18) are analyzed using the L^2 error norm.

Effects of Point Distribution. To demonstrate how well reconstruction algorithms perform with varying point distribution accompanied by our shape reconstruction algorithm. Normally, four different scenarios are considered for this comparison task, DBDI (dense boundary dense internal), DBSI (dense boundary sparse internal), SBDI (sparse boundary dense internal) and SBSI (sparse boundary sparse internal), see Figure 19.

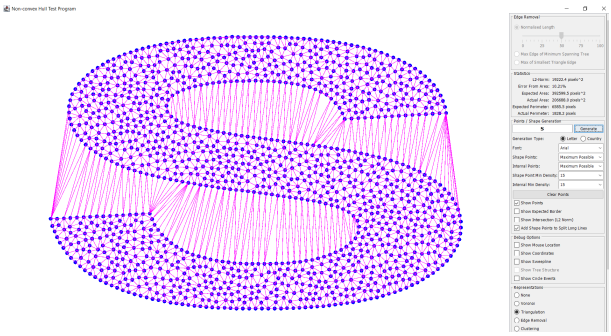

Figure 20: Chi shape software interface.

4.2. Software Tools and Data

- *chi*-shape Software: *chi*-shap algorithm helps to generate non-convex simple polygons for sets of points in the plane. The software can be downloaded at http://duckham.org/matt/characteristics-shapes/.
  This software is available in two versions: a Java Web Start (JWS) version and a full Java jar file. The software has several sections (see Figure 20) which help users to generate different shapes and structures. Users can generate point sets of English alphabets as well as the country maps. The statistics column of the software maintains parameters such as L^2-Norm, error from area, expected area, actual area, expected perimeter, and actual perimeter. The edge removal section focuses on generating customized shapes based on normalized length or maximum edge of minimum spanning tree or maximum of smallest triangle edge. Some edge removal options help users to remove edges and show internal triangles thereby helping the user to customize shapes and error elimination. Figure 21 illustrates some customized shapes and representations.

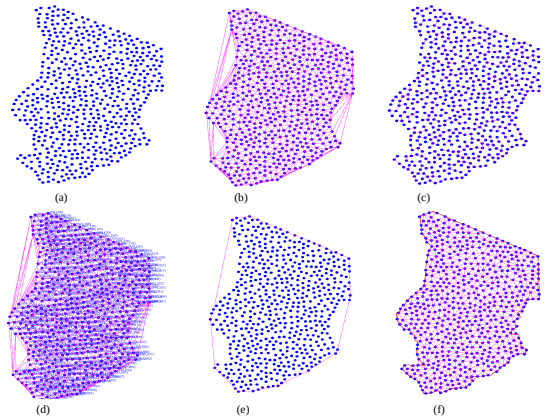

Figure 21: Data generation and various visualization options available in Chi shape software (a) Random generated shape, (b) Delaunay triangulation, (c) Minimum spanning tree (d) Debug option showing coordinates, (e) Convexhull (f) Generated final border.

- CGAL Library [CGA12]: An implementation of alpha shapes is available in Computational Geometry Algorithms Library (CGAL) [CGA12], see https://doc.cgal.org/latest/Alpha_shapes_2/index.html. CGAL *alpha* shapes are built on Delaunay triangulation. The implementation allows the users to generate *alpha*-complex, i.e., a sub-complex of $DT(S)$ which contains *alpha*-exposed k-simplicies with k ranging in the interval $(0,d)$.
- Other Software: Open source implementations of a few other algorithms are available, please see Table 2. Most algorithms are implemented in C++ using geometric predicates available in Computational Geometric Algorithms Library.

Acknowledgement

The materials provided in this course notes are compiled or reproduced from the following papers and theses: [EKS83], [Ede98], [DKWG08b], [GD06], [Pee15], [PM15a], [MPM15], [TPM20], [TPM21].

References

[ABE98] AMENTA N., BERN M., EPPSTEIN D.: The crust and the beta-skeleton: Combinatorial curve reconstruction. *Graphical Models and Image Processing 60*, 2 of 2 (1998), 125–135. 5, 6

[Att98] ATTALI D.: r-regular shape reconstruction from unorganized points. *Computational Geometry 10*, 4 (1998), 239 – 247. Special Issue on Applied Computational Geometry. 6

[CCP97] CHAUDHURI A., CHAUDHURI B., PARUI S.: A novel approach to computation of the shape of a dot pattern and extraction of its perceptual border. *Computer Vision and Image Understanding 68*, 3 (1997), 257 – 275. 1, 3

[CDS13] CHENG S.-W., DEY T. K., SHEWCHUK J. R.: *Delaunay Mesh Generation*. Chapman and Hall / CRC computer and information science series. CRC Press, 2013. 3

[CGA12] CGAL: Computational geometry algorithms, http://www.cgal.org/, December 2012. URL: http://www.cgal.org/. 10

[CM11] CHEVALLIER N., MAILLOT Y.: Boundary of a non-uniform point cloud for reconstruction: Extended abstract. In *Proceedings of the Twenty-seventh Annual Symposium on Computational Geometry* (New York, NY, USA, 2011), SoCG '11, ACM, pp. 510–518. URL: http://doi.acm.org/10.1145/1998196.1998278, doi:10.1145/1998196.1998278. 2

[DKWG08a] DUCKHAM M., KULIK L., WORBOYS M., GALTON A.: Efficient generation of simple polygons for characterizing the shape of a set of points in the plane. *Pattern Recogn. 41* (October 2008), 3224–3236. URL: http://portal.acm.org/citation.cfm?id=1385702.1385955, doi:10.1016/j.patcog.2008.03.023. 2, 8, 9

[DKWG08b] DUCKHAM M., KULIK L., WORBOYS M., GALTON A.: Efficient generation of simple polygons for characterizing the shape of a set of points in the plane. *Pattern recognition 41*, 10 (2008), 3224–3236. 4, 10

[Ede98] EDELSBRUNNER H.: Shape reconstruction with delaunay complex. In *Proceedings of the Third Latin American Symposium on Theoretical Informatics* (London, UK, UK, 1998), LATIN '98, Springer-Verlag, pp. 119–132. 1, 3, 10

[EKS83] EDELSBRUNNER H., KIRKPATRICK D., SEIDEL R.: On the shape of a set of points in the plane. *Information Theory, IEEE Transactions on 29*, 4 (July 1983), 551 – 559. doi:10.1109/TIT.1983.1056714. 2, 3, 4, 8, 10

Sl. No	Algorithm	URL
1	CT-shape	https://github.com/agcl-mr/Reconstruction-CTShape
2	Petal ratio	https://github.com/agcl-mr/Reconstruction-Discern
3	Shape-hull graph	https://github.com/jijup/Shapehull2D
4	EC-shape	https://github.com/ShyamsTree/HoleDetection

Table 2: A few open source implementations of shape reconstruction algorithms.

[EM94] EDELSBRUNNER H., MÜCKE E. P.: Three-dimensional alpha shapes. *ACM Trans. Graph. 13*, 1 (jan 1994), 43–72. URL: https://doi.org/10.1145/174462.156635, doi:10.1145/174462.156635. 3

[Fed59] FEDERER H.: Curvature measures. *Transactions of the American Mathematical Society 93*, 3 (1959), 418–491. 7

[Fis] FISCHER K.: Introduction to alpha shapes. *Report*. URL: https://graphics.stanford.edu/courses/cs268-11-spring/handouts/AlphaShapes/as_fisher.pdf. 3, 4

[GC99] GARAI G., CHAUDHURI B. B.: A split and merge procedure for polygonal border detection of dot pattern. *Image and Vision Computing 17*, 1 (1999), 75 – 82. URL: http://www.sciencedirect.com/science/article/B6V09-3VPB718-8/2/90627923ed9c18b9c430307830ffb55e, doi:DOI:10.1016/S0262-8856(98)00089-4. 3

[GD06] GALTON A., DUCKHAM M.: What is the region occupied by a set of points? In *Geographic Information Science*, Raubal M., Miller H., Frank A., Goodchild M., (Eds.), vol. 4197 of *Lecture Notes in Computer Science*. Springer Berlin / Heidelberg, 2006, pp. 81–98. 10.1007/118639396. URL: http://dx.doi.org/10.1007/118639396. 1, 2, 10

[GDJ*11] GHEIBI A., DAVOODI M., JAVAD A., PANAHI F., AGHDAM M., ASGARIPOUR M., MOHADES A.: Polygonal shape reconstruction in the plane. *Computer Vision, IET 5*, 2 (march 2011), 97 –106. doi:10.1049/iet-cvi.2009.0079. 3, 8

[GRM15] GANAPATHY H., RAMU P., MUTHUGANAPATHY R.: Alpha shape based design space decomposition for island failure regions in reliability based design. *Structural and Multidisciplinary Optimization 52* (2015), 121–136. 1

[GS69] GABRIEL K. R., SOKAL R. R.: A new statistical approach to geographic variation analysis. *Systematic Zoology 18*, 3 (1969), pp. 259–278. 2

[JT92] JAROMCZYK J., TOUSSAINT G.: Relative neighborhood graphs and their relatives. *Proceedings of the IEEE 80*, 9 (sep 1992), 1502 –1517. doi:10.1109/5.163414. 2

[KPV10] KRASNOSHCHEKOV D. N., POLISHCHUK V., VIHAVAINEN A.: Shape approximation using k-order alpha-hulls. In *Proceedings of the 2010 annual symposium on Computational geometry* (New York, NY, USA, 2010), SoCG '10, ACM, pp. 109–110. 2

[KR85] KIRKPATRICK D. G., RADKE J. R.: A framework for computational morphology. *Computational Geometry, ed. G. T. Toussaint* (1985), 217–248. 2

[MD00] MELKEMI M., DJEBALI M.: Computing the shape of a planar points set. *Pattern Recognition 33*, 9 (2000), 1423 – 1436. URL: http://www.sciencedirect.com/science/article/pii/S0031320399001247, doi:https://doi.org/10.1016/S0031-3203(99)00124-7. 2, 4

[MKPM17] METHIRUMANGALATH S., KANNAN S. S., PARAKKAT A. D., MUTHUGANAPATHY R.: Hole detection in a planar point set: An empty disk approach. *Computers & Graphics 66* (2017), 124–134. 2

[MPM15] METHIRUMANGALATH S., PARAKKAT A. D., MUTHUGANAPATHY R.: A unified approach towards reconstruction of a planar point set. *Computers & Graphics 51* (2015), 90–97. 2, 6, 7, 8, 10

[MS07] MOREIRA A. J. C., SANTOS M. Y.: Concave hull: A k-nearest neighbours approach for the computation of the region occupied by a set of points. In *GRAPP (GM/R)* (2007), Braz J., Vázquez P.-P., Pereira J. M., (Eds.), INSTICC - Institute for Systems and Technologies of Information, Control and Communication, pp. 61–68. 2

[OPP*21] OHRHALLINGER S., PEETHAMBARAN J., PARAKKAT A. D., DEY T. K., MUTHUGANAPATHY R.: 2d points curve reconstruction survey and benchmark. *Computer Graphics Forum 40*, 2 (2021), 611–632. 1

[O'R94] O'ROURKE J.: *Computational Geometry in C*. Cambridge University Press, New York, NY, USA, 1994. 4

[O'R98] O'ROURKE J.: *Computational Geometry in C*, 2nd ed. Cambridge University Press, New York, NY, USA, 1998. 2

[Pee15] PEETHAMBARAN J.: Non-parametric shape reconstruction and volume constrained polyhedronizations of point sets, 2015. 10

[PM15a] PEETHAMBARAN J., MUTHUGANAPATHY R.: A non-parametric approach to shape reconstruction from planar point sets through delaunay filtering. *Computer-Aided Design 62* (2015), 164–175. 1, 2, 5, 6, 8, 10

[PM15b] PEETHAMBARAN J., MUTHUGANAPATHY R.: A non-parametric approach to shape reconstruction from planar point sets through delaunay filtering. *Computer-Aided Design 62* (2015), 164 – 175. 7

[PMM18] PARAKKAT A. D., METHIRUMANGALATH S., MUTHUGANAPATHY R.: Peeling the longest: A simple generalized curve reconstruction algorithm. *Computers & Graphics 74* (2018), 191 – 201. 7

[SCT*14] SUNDAR B. R., CHUNDURU A., TIWARI R., GUPTA A., MUTHUGANAPATHY R.: Footpoint distance as a measure of distance computation between curves and surfaces. *Computers & Graphics 38* (2014), 300–309. URL: https://www.sciencedirect.com/science/article/pii/S0097849313001738, doi:https://doi.org/10.1016/j.cag.2013.10.032. 1

[Tou88] TOUSSAINT G.: A graph-theoretical primal sketch. *Computational Morphology* (1988), 229–260. 2

[TPM20] THAYYIL S. B., PARAKKAT A. D., MUTHUGANAPATHY R.: An input-independent single pass algorithm for reconstruction from dot patterns and boundary samples. *Computer Aided Geometric Design 80* (2020), 101879. 2, 7, 10

[TPM21] THAYYIL S. B., PEETHAMBARAN J., MUTHUGANAPATHY R.: A sampling type discernment approach towards reconstruction of a point set in r2. *Computer Aided Geometric Design 84* (2021), 101953. 7, 8, 9, 10

[Vel94] VELTKAMP R. C.: *Closed Object Boundaries from Scattered Points*. Springer-Verlag New York, Inc., Secaucus, NJ, USA, 1994. 2

[XFZQ10] XU J., FENG Y., ZHENG Z., QING X.: A concave hull algorithm for scattered data and its applications. In *Image and Signal Processing (CISP), 2010 3rd International Congress on* (oct. 2010), vol. 5, pp. 2430 –2433. doi:10.1109/CISP.2010.5648277. 2